Earth and Planetary Science Letters 400 (2014) 45–53

Contents lists available at ScienceDirect

Earth and Planetary Science Letters

www.elsevier.com/locate/epsl

Shear-velocity structure of the Tyrrhenian Sea: Tectonics, volcanism and mantle (de)hydration of a back-arc basin

Sonja Greve [a,1], Hanneke Paulssen [a,*], Saskia Goes [b], Manfred van Bergen [a]

[a] Dept. of Earth Sciences, Utrecht University, Utrecht, The Netherlands
[b] Dept. of Earth Science and Engineering, Imperial College London, London, UK

ARTICLE INFO

Article history:
Received 29 January 2014
Received in revised form 16 May 2014
Accepted 18 May 2014
Available online xxxx
Editor: P. Shearer

Keywords:
Tyrrhenian Sea
surface waves
tomography
back-arc basin
asthenosphere
hydration

ABSTRACT

The Tyrrhenian Sea in the Mediterranean formed as the result of roll-back of the Adriatic and Ionian subducting plates. It is mostly underlain by strongly thinned continental lithosphere, but contains two small oceanic basins in the southern Tyrrhenian, the youngest one located just behind the active magmatic arc. Its regional setting with dense station coverage provides a unique opportunity to derive a high-resolution, 3-D shear-velocity model of this back-arc basin and surrounding onshore areas using interstation Rayleigh-wave dispersion measurements. Our tomographic model, extending to a depth of approximately 160 km, displays a pronounced, nearly ring-shaped low shear-velocity zone between 70 and 110 km depth which surrounds the older oceanic Vavilov Basin. The sharp velocity decrease at 70 km depth can be explained by the transition from a relatively dry lithospheric mantle to more hydrous asthenospheric mantle material. The tectonic evolution of the region and the correlation of the low-velocity anomaly with subduction-related volcanism indicate that the low-velocity anomaly reflects hydrous mantle material in (present or former) mantle wedge regions. We suggest that the absence of the low-velocity zone beneath the Vavilov Basin is due to mantle dehydration caused by the creation of MORB crust. Whereas temperature effects may dominate the asthenospheric shear-velocity differences between various back-arc basins, we find that the variations in shear-velocity structure within the Tyrrhenian area are best explained by variations in mantle water content.

1. Introduction

The Tyrrhenian Sea is a back-arc basin in the Mediterranean Sea which formed within the general framework of convergence of Africa and Eurasia. There is general agreement that much of the evolution of the western Mediterranean is governed by several stages of slab roll-back (e.g., Malinverno and Ryan, 1986; Dewey et al., 1989; Gueguen et al., 1998; Wortel and Spakman, 2000; Faccenna et al., 2004; Rosenbaum and Lister, 2004; Faccenna et al., 2007; Jolivet et al., 2009). In the first major stage, from 30 to 15 Ma, Corsica and Sardinia were separated from the European mainland by counterclockwise rotation leading to the opening of the Liguro-Provinçal and Valencia basins. The Tyrrhenian Sea was formed during the second major stage, from 15 Ma to Present. Initially it opened by east–west rifting, driven by the Adriatic slab, along the western margin of Corsica and Sardinia. The northern Tyrrhenian Sea, roughly corresponding to latitudes larger than 41°N, opened at a relatively slow rate (~1–1.5 cm/yr). The opening of the southern Tyrrhenian Sea is the result of enhanced extension by roll-back of the Adriatic–Ionian slab system towards the southeast. This happened in two steps with the formation of the Vavilov Basin occurring during the first episode (8–4 Ma) (e.g., Argnani and Savelli, 1999; Faccenna et al., 2007). The Marsili Basin, surrounded by the currently active Aeolian island arc, opened during the second episode (2–1 Ma).

Volcanism of the Tyrrhenian Sea and its surroundings shows remarkably large variations in time and space reflecting the complex tectonic evolution of the region. The petrological and geochemical signatures of the subduction-related (ranging from calc-alkaline to shoshonitic and ultra-potassic), intraplate and mid-ocean-ridge-type magmatism point to large differences in mantle source compositions and degrees of melting (e.g., Savelli, 2002; Peccerillo, 2005; Lustrino et al., 2011). The compositional characteristics of volcanism of the last 14 Myr as well as of samples from deep drill holes are depicted in Fig. 1.

The geochemical signatures of the subduction-related magmas require a heterogeneous mantle source, likely including lithospheric- or wedge-mantle material that has been variably metasomatized by fluids derived from continental and oceanic slabs

* Corresponding author.
E-mail address: h.paulssen@uu.nl (H. Paulssen).
[1] Presently at: CGG Services (Norway) AS, Oslo, Norway.

http://dx.doi.org/10.1016/j.epsl.2014.05.028

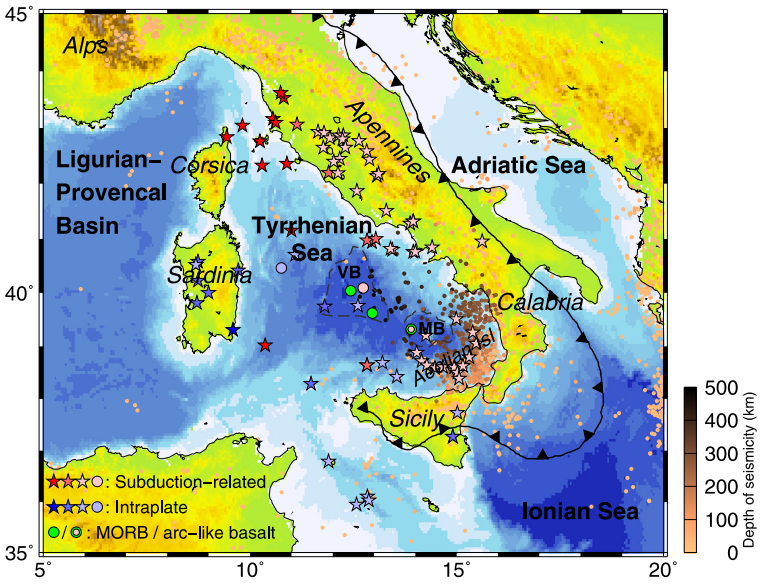

Fig. 1. Tectonic map of the larger Tyrrhenian Sea area. The plate boundary along the Adriatic and Ionian arc is shown as thick black line with triangles indicating the sense of subduction. The Vavilov Basin (VB) and Marsili Basin (MB) are outlined by dashed lines. Volcanic centres are indicated by stars and samples from deep drill holes by outlined circles. Different rock types are represented by different colours: Subduction-related in red (14–4 Ma), dark pink (4–2 Ma) and light pink (2–0 Ma); Intraplate in blue (14 Ma), lighter blue (4–2 Ma) and light blue (2–0 Ma). Samples from deep drill holes with MORB (4–3 Ma) and arc-like basalt (2–0 Ma) are depicted in green and combined green/pink, respectively. Brown circles indicate seismicity. Sources for volcanism are Savelli (2002), Peccerillo (2005) and Lustrino et al. (2011). (For interpretation of the references to colour in this figure legend, the reader is referred to the web version of this article.)

(for an overview see Peccerillo, 2005). The subduction-related volcanism in the northern Tyrrhenian Sea shows an eastward age decrease which can be related to roll-back of the Adriatic plate in an eastward direction. The geochemical signature of recent potassium-rich volcanism in central Italy is associated with past subduction of the continental Adriatic slab. In large parts of peninsular Italy, volcanic activity postdates the timing of subduction or metasomatism, and may have been initiated by later changes in mantle conditions, possibly caused by slab detachment and the subsequent opening of a slab window (Bianchini et al., 2008; Rosenbaum et al., 2008; Nikogosian and Van Bergen, 2010). On the other hand, the current, mostly calc-alkaline, volcanism of the Aeolian arc is associated with active subduction of the oceanic Ionian plate.

In the southern Tyrrhenian Sea, intraplate volcanism as well as mid-ocean ridge basalts (MORBs) recovered from two deep ocean drill holes in the oceanic Vavilov Basin are not directly associated with subduction. Instead, they are likely generated by extension in a back-arc setting, producing upwelling and decompression melting of mantle material.

In spite of the fact that the Tyrrhenian Sea is an extensively studied area, much of the upper mantle seismic structure beneath the Tyrrhenian Sea is still poorly resolved. The station distribution on land inhibits proper illumination of the shallow Tyrrhenian mantle by tomographic studies that use teleseismic P- and S-wave arrival times (e.g., Lucente et al., 1999; Piromallo and Morelli, 2003; Spakman and Wortel, 2004; Di Stefano et al., 2009; Giacomuzzi et al., 2011, 2012). Studies using surface waves (Panza et al., 2007; Schivardi and Morelli, 2011) or waveform modelling (Schmid et al., 2008; Zhu et al., 2012), on the other hand, suffer from large source–receiver distances with additional sensitivity outside the area of interest. In this study we therefore used the two-station method to reduce the surface wave propagation effects from the event to the most nearby station.

We measured interstation Rayleigh-wave phase velocities, which were inverted to model the upper-mantle ($<$ 200 km) shear-velocity structure. Linking the seismic model to the volcanics and tectonic evolution of the region, we infer that subduction-induced mantle hydration, as well as mantle dehydration caused by extension and the formation of new oceanic crust, have been instrumental for the present state and composition of the Tyrrhenian upper mantle.

2. Data and interstation phase-velocity measurements

We used the two-station method as developed by Meier et al. (2004) to determine the upper-mantle shear-velocity structure beneath the Tyrrhenian Sea. The two-station method is a technique to determine the surface-wave phase velocity between two stations by cross-correlation. In case of an event located along a great circle connecting two recording stations, it assumes that the phase difference between the stations is mainly caused by the structure along the interstation path (De Vos et al., 2013). Compared to the more commonly used source–receiver geometries, surface wave interstation measurements often have the advantage of a closer spacing, providing a higher lateral resolution.

The two-station method relies on event–station constellations which provide a good path coverage of the study region and good azimuthal coverage to decrease finite frequency effects. Thus, we examined data from teleseismic and regional earthquakes recorded at 386 stations over a period of more than a decade (07/1995–06/2009). The chosen stations are part of temporary (CATSCAN, MIDSEA, RETREAT) and permanent (MEDNET, Italian National Seismic Network, French BB, GEOFON, IMS) networks in Italy, southern France, Corsica and Tunisia. All seismographs are corrected for instrument response and downsampled to 1 s before phase velocities are measured.

We measured interstation phase velocities of fundamental-mode Rayleigh waves from the phase of the cross-correlation function of two vertical component seismograms for events taken within 7° of the interstation azimuth. The cross-correlation function is filtered with a set of frequency-dependent Gaussian band-pass filters and windowed in the time domain to suppress effects from other signals. To avoid multiple-cycle ambiguities each curve is individually picked by comparing to a reference phase-velocity curve. Only smooth segments of the phase-velocity curves are selected, to avoid irregularities which could be artifacts from finite-frequency effects. For each interstation path, the measured dispersion curves were averaged to obtain the final path-averaged

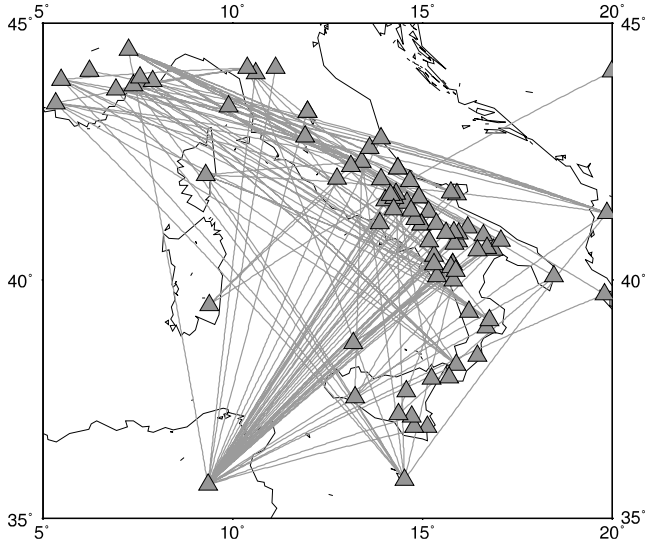

Fig. 2. Interstation raypath coverage.

fundamental-mode phase-velocity curve. Using events from different directions and distances helps to minimize effects from non-plane waves and off-great-circle paths. Measurements were discarded if the dispersion curves from events from opposite directions were inconsistent. Finally, some dispersion curves, which appeared to deviate from the general trend and which are potentially related to multipathing, were also excluded. In the final data set the number of event dispersion curves contributing to a single interstation curve is on average 14, ranging from 4, for only a few paths with very coherent dispersion curves, to 97. The applied extensive and thorough data selection assured a high quality and reliable data set as base for the tomographic inversion and the influence of non-plane waves and uncorrelated noise on the final dispersion curves is considered small (see also Pedersen, 2006). The final data set consists of up to 127 interstation paths from 77 stations (Fig. 2), although the actual number of interstation measurements per frequency may be lower (for a figure of the number of data per frequency, see supplementary material).

3. Construction of phase-velocity maps

To construct the phase-velocity maps for various periods, we inverted the interstation phase-velocity data on a triangular grid of 200 nodes with a spacing of about 70 km. The inversions were performed using LSQR (Paige and Saunders, 1982) with smoothing and damping parameters large enough not to overinterpret the data and small enough not to miss important stable structural details. Stability of the inversion results was verified by the small sensitivity of the phase-velocity maps to small variations of the regularization parameters, as well as a good recovery of predefined input patterns. Furthermore, resolution matrices were calculated to assess trade-offs or lateral smearing from one node to its neighbours. Further details on resolution are given below. The regularization parameters were taken the same for the phase-velocity maps of all periods to avoid changes in resolution due to variations in regularization.

We computed phase-velocity maps at 19 periods from 10 to 200 s. The period range with good data coverage and resolution spans 25–130 s, which is broad enough to image structure from the middle crust to the upper asthenosphere. Fig. 3 shows examples for periods of 25, 50, 80 and 130 s. For a period of 25 s the imaged features largely correspond to variations in the crustal structure of the region. The most obvious feature is the sharp contrast along the coastline of the Italian peninsula which reflects the increase in crustal thickness from the Tyrrhenian Sea to the Italian mainland. At a period of 50 s the distinction between oceanic and continental areas disappears and the magnitudes of phase-velocity anomalies become smaller. Low-velocity regions are found below the western coast of mainland northern Italy, for an area in central Italy, Corsica and the northern tip of Sicily. A distinct high-velocity area defines the central Tyrrhenian Sea. The 80 s phase-velocity map shows an extended low-velocity region covering most of the Tyrrhenian Sea as well as Corsica, Sardinia, Northern Apennines and Sicily. In the 130 s phase-velocity map this low-velocity region even extends further southeast in the Tyrrhenian Sea.

Resolution matrices were calculated to estimate the robustness of our phase-velocity maps (see supplementary material). The diagonal elements in the resolution matrix provide a measure of the amount of recovery, or resolution, at each of the nodes, whereas the non-diagonal elements provide a measure of the amount of lateral smearing. For the results shown here, we consider a value of 0.3 or higher on the diagonal as high resolution (areas within green contour in Figs. 3 and 4). In general, one to two nodes are affected by smearing, corresponding to a distance of 70–140 km.

To illustrate the robustness of the results in a more intuitive way, we performed resolution tests by inverting a synthetic model using the same data coverage and regularization parameters. The synthetic model consists of circular low-velocity anomalies (−2.55%) embedded in a high-velocity environment (+2.55%) (Fig. 4e). The results from this resolution test are shown in Figs. 4a–d. In general, the areas of good resolution as determined from the resolution matrix correspond to areas where the input perturbation patterns are recovered in shape. The amplitudes are only recovered by roughly 50% (the central anomaly by 67%). Outside these areas, the circular shapes of the anomalies smear out and the recovery of structures diminishes.

4. Shear-velocity inversion

Phase-velocity maps (Fig. 4) provide the local Rayleigh phase-velocity dispersion curve for each geographical grid point of the map. Each of these dispersion curves is inverted individually for 1D shear-velocity structure at the grid point. The 1D velocity profiles are then combined to create a 3D shear-velocity model. The inversion is performed by means of a damped iterative linearised optimisation. In the inversion P-wave velocity and density are kept in a constant ratio to the shear-wave velocity as Rayleigh-wave phase velocity is mainly sensitive to shear-wave velocity.

As the phase-velocity sensitivity for periods of 10 s or more (as used in our study) is insufficient to well resolve crustal structure, the starting model should already contain reliable crustal thicknesses. We used the EPcrust model from Molinari and Morelli (2011) for the crustal structure which is based on a comprehensive compilation of previous crustal models. This is supplemented by the AK135 model (Kennett et al., 1995) for the deeper mantle sections. The parameterisation of the model space consists of 20 basis functions (14 layers spanning the crust and mantle to 210 km, and 6 wider and deeper triangular basis functions) to describe the shear-wave velocity structure down to 1000 km. The inversion for the deeper structures is included to avoid leakage from (otherwise fixed) deeper structures into the shallow structure. In addition, three parameters allow the inversion for depth perturbations of Moho, 410-km and 660-km discontinuities.

Fig. 5 shows the crustal thickness and the shear-velocity anomaly with respect to reference model AK135 from 40 to 160 km depth. In this depth range this reference model has a nearly constant, only slightly increasing, shear velocity of approximately 4.5 km/s. The shear-velocity model is not shown for larger depths because of reduced depth resolution of our data. The results of the inversion regain the Moho depth of the initial starting

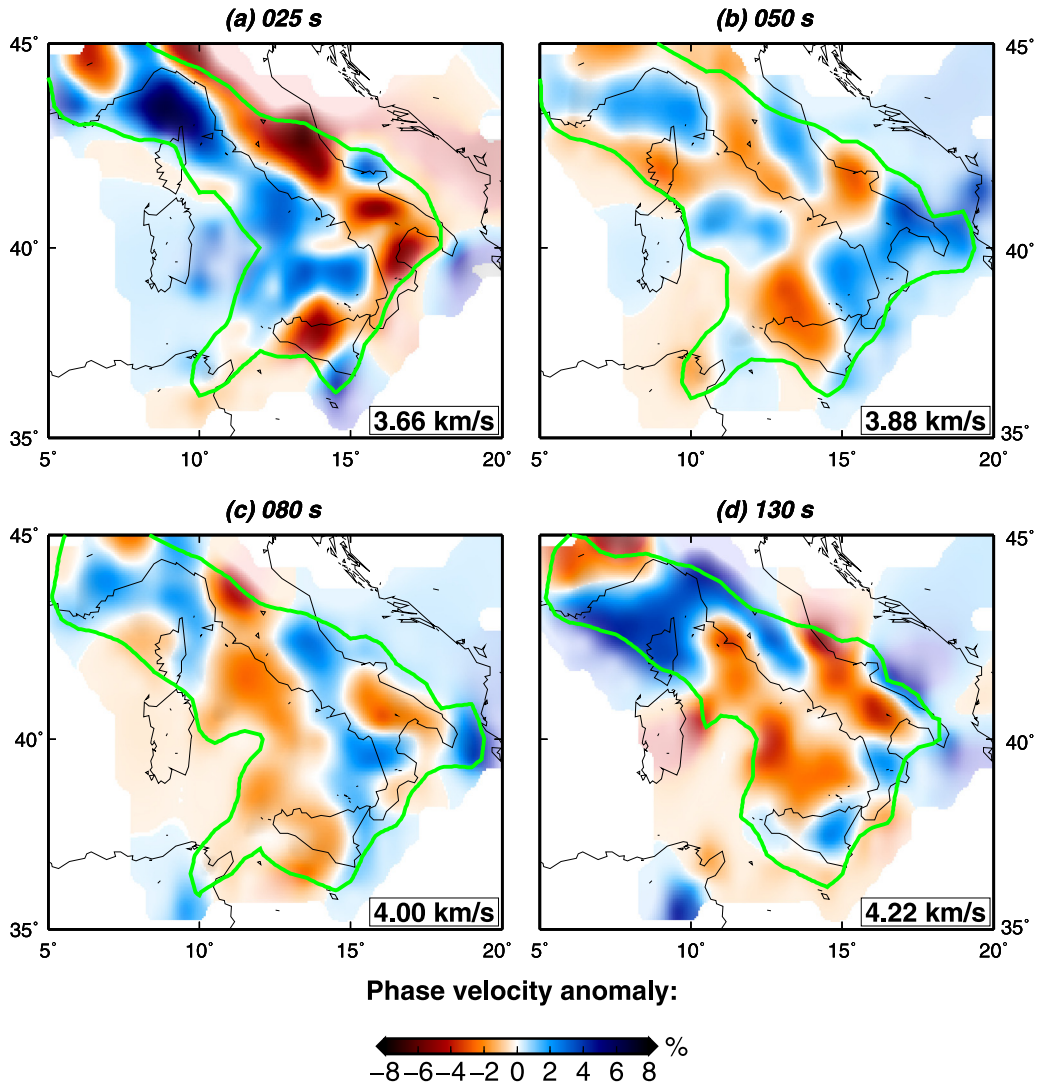

Fig. 3. Rayleigh-wave phase-velocity maps for periods of 25 s, 50 s, 80 s and 130 s. Colours indicate velocity anomalies relative to an average reference phase velocity as given in the lower right corner of each map. The green contour line in each map surrounds the area of good resolution, where the diagonal element of the resolution matrix is larger than 0.3. The areas outside this contour are faded. (For interpretation of the references to colour in this figure legend, the reader is referred to the web version of this article.)

model with some expected smoothing, but with a sufficient accuracy (Fig. 5, top panel). At 40 km, a few strong low-velocity anomalies appear in the shear-velocity map. In these areas crustal thickness exceeds 40 km, so that the crustal velocities show up as pronounced anomalies compared to the prevailing mantle velocities at this depth. At 50 and 60 km depth, the shear-velocity structure becomes more uniform and shows few variations. However, a faint pattern is apparent at these depths and develops into the most striking observation in the velocity structure at 80 km depth. A strong nearly ring-shaped low-velocity region covers the arc region of the Calabrian and Ionian subduction, the island of Corsica and the onshore parts of northern Italy. Going deeper to 120 km, this pattern fades out and nearly reverses at 160 km depth, where the lowest velocities are found beneath central Tyrrhenian Sea and offshore Sardinia. The more homogeneous velocity structure can be partly due to lack of resolution at greater depths. Furthermore, the resolution in the area of Sardinia and its southeastern extension is insufficient due to the poor path coverage (see Figs. 2 and 4).

To confirm the stability of the inversion results, tests were performed with a variety of different inversion parameters. The starting model may have an influence on the final velocity model, and, in particular, the crustal structure of the starting model may affect the underlying mantle structure. Thus, for one set of tests we modified the starting models. We implemented a minor change by adjusting the crustal structure to EuCRUST-07 (Tesauro et al., 2008), but we also defined a constant oceanic or continental velocity profile for each grid point, and finally we changed the value of the constant mantle velocity. For all of these tests, the nearly ring-shaped anomaly remained the dominant feature, although the resolution of the Moho diminished. In additional tests the Moho depth was fixed, and less basis functions were used to parameterise the model space. Also, for these tests the nearly ring-shaped anomaly could still be identified but with some loss of depth resolution. Fig. 6 shows two shear velocity profiles to illustrate the depth dependence, one for a grid point in the northern Tyrrhenian close to the Italian mainland and another one for a grid point in the Vavilov Basin. The velocity profile for the Vavilov Basin has a near-constant mantle velocity of around 4.4 km/s whereas the northern Tyrrhenian Sea shows a velocity decrease at around 60 km depth. The velocity decrease at other points can more pronounced, for instance decreasing to 4.1 km/s in the northern Tyrrhenian east of Sardinia.

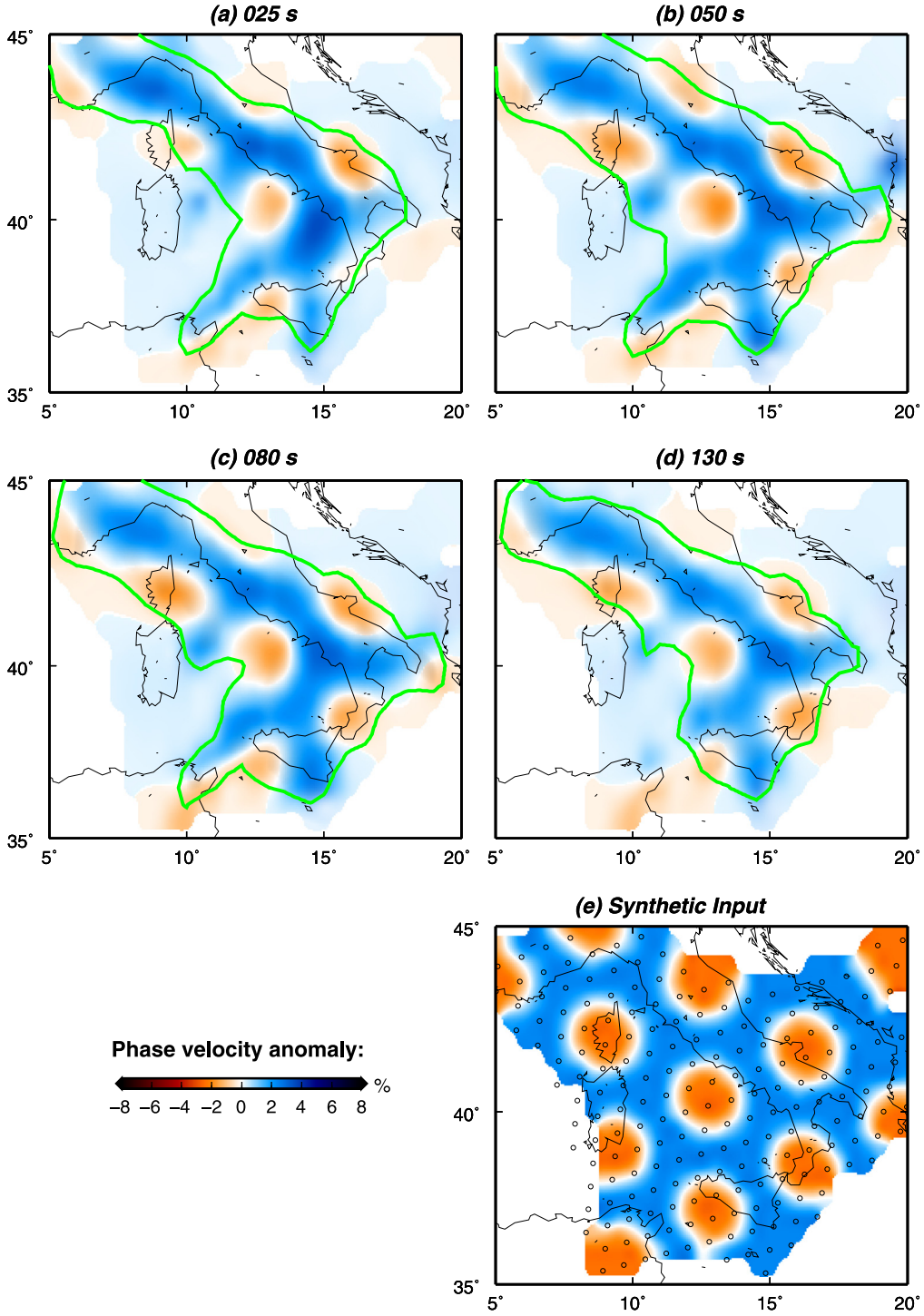

Fig. 4. Resolution test for a synthetic input model with circular low-velocity areas within the study area (panel e). Inversions are performed for the same periods and with the same parameters as for the results shown in Fig. 3. (For interpretation of the references to colour in this figure, the reader is referred to the web version of this article.)

The low-velocity anomaly at 80 km, which more or less surrounds the centre of Tyrrhenian Sea, was not anticipated on the basis of a simple geodynamic model of lithospheric extension caused by rollback. For such a scenario, a shear-velocity model with the lowest velocities would be expected in the region of largest extension (the central Tyrrhenian Sea) due to asthenospheric upwelling. Previous seismic studies, however, are in agreement with our results. The results of the study by Marone et al. (2004) for the Mediterranean have less resolution, but show a similar pattern. Furthermore, for the Tyrrhenian Sea there is good agreement with the study by Zhu et al. (2012) who performed a waveform inversion of frequency dependent body and surface waves for the entire European upper mantle using an adjoint tomographic technique. The agreement with the surface wave study of Panza et al. (2007) is not so good at a few locations, but it is somewhat difficult to compare their results to our model because of their cellular representation.

A comparison with tomographic studies of P- or S-wave travel times is not straightforward due to the differences in illumination. Given the station distribution on land, tomographic travel-

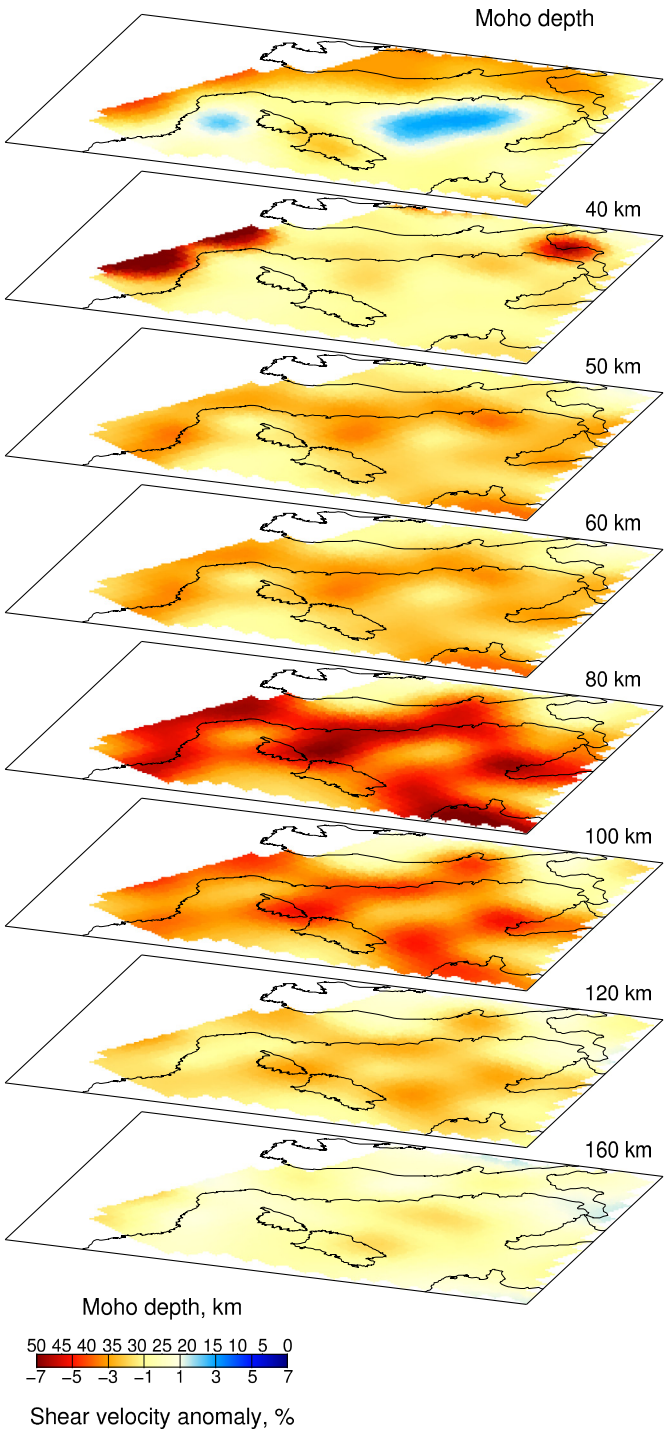

Fig. 5. 3D shear-wave velocity model. Top panel: Map of the crustal thickness. Lower panels: Shear-wave anomalies relative to the global reference model AK135 at depths of 40, 50, 60, 80, 100, 120 and 160 km.

time studies better image the subducting slabs than this study, while lacking resolution in the shallow part of the upper mantle of Tyrrhenian Sea. Furthermore, in general, the body wave studies have a better lateral resolution, whereas the surface-wave studies have a better vertical resolution in the uppermost mantle. Despite these differences, there is a fairly good agreement in terms of the location of the broad-scale slow and fast anomalies between our study and the S-wave tomographic study by Giacomuzzi et al. (2012) for the Italian mainland, and an even better qualitative agreement with the P-wave tomographic results of Piromallo and Morelli (2003) and Spakman and Wortel (2004).

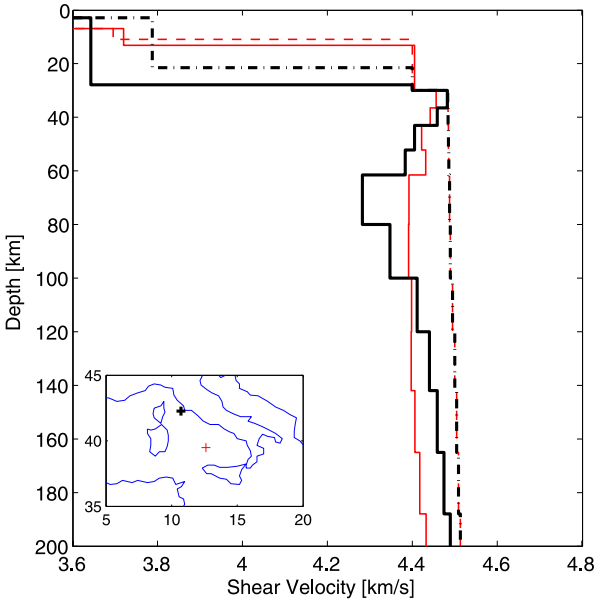

Fig. 6. Shear-velocity structure for a grid point in the northern Tyrrhenian Sea (thick black) and Vavilov Basin (thin red). Dashed and dash-dotted lines show the starting models for the inversion with varying crust and AK135 mantle structure. (For interpretation of the references to colour in this figure legend, the reader is referred to the web version of this article.)

5. Interpretation

The shear-velocity model of the Tyrrhenian Sea area shows strong lateral variations in the upper mantle that are related to its complex tectonic history. The most striking feature is the nearly ring-shaped pronounced low-velocity anomaly over a depth range from roughly 70 to 110 km with minimum shear velocity at approximately 80 km. In order to address the nature and origin of this low-velocity anomaly, we must explain both the vertical extent of the anomaly as well as its pattern.

Although a low-velocity zone with a minimum shear-velocity of 4.1 km/s as found here does not necessarily require the presence of melts or fluids (Stixrude and Lithgow-Bertelloni, 2005; Faul and Jackson, 2005), models without fluids or melts cannot explain the sharp velocity decrease at 70 km. A strong velocity decrease at similar depths is often observed in oceanic regions and is generally interpreted as the lithosphere–asthenosphere boundary (e.g., Rychert and Shearer, 2009; Fischer et al., 2010; Schmerr, 2012). Oceanic thermal models combined with mineral physics data have shown that the transition from a dry, chemically depleted lithosphere to a hydrated, fertile asthenosphere may be able to produce a quite sharp velocity decrease around the depth where dry melting starts, at approximately 60–70 km (Karato and Jung, 1998; Karato, 2012; Goes et al., 2012). Since water decreases the melting temperature, there could be an additional effect of partial melt, although melt concentrations at these depths are expected to be very small and may not be seismically detectable (e.g., Hirschmann, 2010; Goes et al., 2012).

The Tyrrhenian asthenospheric mantle likely contains water due to past subduction. In the mantle wedge, hydrous fluids are produced by the break-down of minerals carried down by the subduction of the Adriatic and Ionian slabs. Rather than remaining a local effect, slab roll-back in the last 14 Ma may have generated a hydrous mantle zone beneath most of the Tyrrhenian Sea.

Intuitively, one might expect a correlation between the volcanism of the past 14 Ma and the pattern of the low-velocity anomaly at 80 km, but such a correlation is not obvious (Fig. 7). However, by zooming in on the different regions of the area and considering

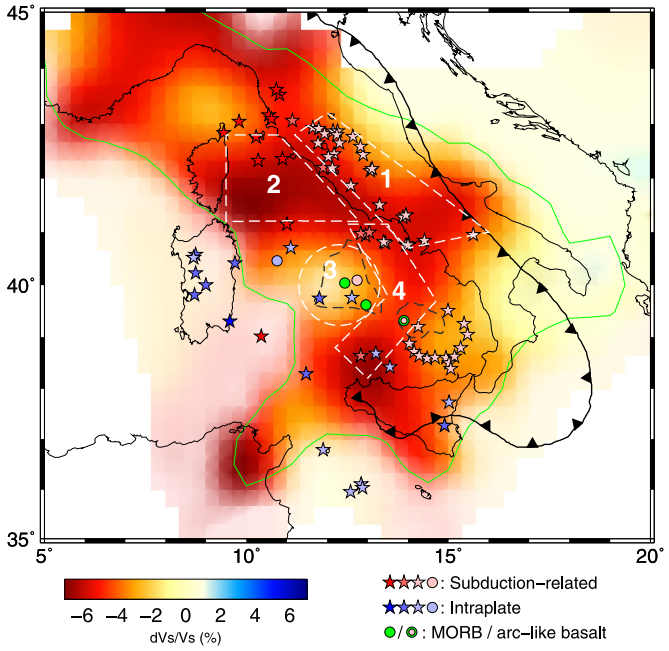

Fig. 7. Shear-wave anomaly (relative to AK135) at a depth of 80 km, and volcanism as in Fig. 1. The regions outlined by the white dashed lines are mentioned in the text. The green contour delineates the area of good resolution, where the diagonal element of the resolution matrix for a period of 50 s is larger than 0.3. The areas outside this contour are faded. (For interpretation of the references to colour in this figure legend, the reader is referred to the web version of this article.)

the tectonic evolution and variations in magmatism, a coherent picture emerges.

The first region (region 1 in Fig. 7) corresponds to the area along the western part of the central Italy peninsula with recent (< 1 Ma) subduction-related volcanism. Although there are compositional differences between the volcanic rocks in this region, their geochemical signatures suggest that they are all generated by partial melting of a lherzolitic mantle metasomatized by various slab components, including H_2O and CO_2 (Peccerillo, 2005; De Astis et al., 2006; Avanzinelli et al., 2009; Frezotti et al., 2009). The low-velocity anomaly therefore likely corresponds to mantle wedge material with fluids and possibly small amounts of melt. However, the timing of magmatic activity (< 1 Ma) in central Italy is not directly linked to subduction of the Adriatic plate which halted at approximately 4 Ma (Goes et al., 2004; Faccenna et al., 2004; Carminati et al., 2010). Based on tomographic evidence showing discontinuity of the Adriatic slab (Lucente et al., 1999; Piromallo and Morelli, 2003; Spakman and Wortel, 2004; Giacomuzzi et al., 2011, 2012), several studies have suggested that volcanism was triggered by slab tearing or break-off (De Astis et al., 2006; Bianchini et al., 2008; Rosenbaum et al., 2008; Nikogosian and Van Bergen, 2010). It is therefore likely that the magmatism in central Italy was initiated by a dynamic cause, such as slab detachment or tearing, which changed the mantle conditions thus allowing previously hydrated mantle to melt.

The northern Tyrrhenian Sea (region 2 in Fig. 7) is an area with clear and pronounced low velocities at 80 km depth. It is also the region of slow (1–1.5 cm/yr) extension due to eastward retreat of the Adriatic slab from 15 to 5 Ma as evidenced by the decreasing age of the subduction-related volcanism from the northern tip of Corsica to Tuscany (Civetta et al., 1978). Low velocities in the 70 to 110 km depth range are expected beneath the northern Tyrrhenian Sea as a consequence of past subduction and slab retreat which produced a mantle enriched in water and other subduction-related components. Note that the lowest shear velocities are found in the area without volcanism. We interpret the very low velocities in region 2 as the expression of subduction-enriched mantle that has not been depleted by melting during the last 5 Myr. The somewhat higher shear velocities around the northern margin of region 2 may, speculatively, be explained by the volcanism in that area, which may have decreased the amount of water and melt.

The distinct low-velocity zone is most notably absent beneath the Vavilov Basin, the region of largest extension of the Tyrrhenian Sea (region 3 of Fig. 7). Here velocities are close to that of reference mantle velocities. Assuming that upwelling caused by extension would produce low seismic velocities by generating decompressional melt, this result may seem paradoxical. However, we argue that the observed shear-velocity pattern of the southern Tyrrhenian Sea matches the evolution of this back-arc basin and its magmatism. Contrary to the northern Tyrrhenian Sea, where extension was accommodated by crustal thinning, the opening of the southern Tyrrhenian Sea was accompanied by oceanic basin formation during two phases of rapid trench retreat (Argnani and Savelli, 1999; Trua et al., 2007; Ventura et al., 2013). During the first period of rapid extension, from 8 to 4 Ma, the Vavilov Basin was created, and after a period of quiescence the Marsili Basin opened between 2 and 1 Ma. Both basins were formed as a consequence of slab retreat, but there is a distinct difference in their crustal composition. Whereas the Vavilov Basin has an (enriched) MORB-like crust, the basaltic crust of the Marsili Basin has a more arc-type affinity (Trua et al., 2007). Although the southern Tyrrhenian supra-slab mantle must have been enriched in water by slab dehydration, the concentration of fluids will have been lower than for the northern Tyrrhenian Sea due to the fast roll-back during the first period of extension, causing a larger influx of mantle material not affected by subduction. A second, probably more important, aspect is that the high degree of melting that produced the MORB crust of Vavilov must have effectively extracted any water out of its mantle source. Thus the mantle below the Vavilov Basin quickly dried out during the formation of its oceanic crust, while fast slab rollback precluded rehydration, leaving a higher-velocity asthenosphere. As a result of these two aspects, a less hydrous mantle is expected below the Vavilov Basin compared to the surrounding areas. We therefore suggest that the relatively normal shear velocity at a depth of 80 km reflects a relatively dry Tyrrhenian mantle.

The episode of rapid extension and Vavilov Basin formation was followed by a period without significant roll-back during Pliocene (5–2 Ma). During this period a submerged arc was formed around the Vavilov Basin which produced calc-alkaline volcanism from offshore Italy, to the northwestern tip of Sicily (Argnani and Savelli, 1999). This arc now separates the Marsili and Vavilov Basins and can be identified by a higher elevation and larger Moho depth compared to these basins. Notably, its location matches the region of low velocities from the Italian mainland to Sicily (region 4 in Fig. 7). It is therefore likely that this low-velocity anomaly represents the hydrous mantle wedge of this former subduction-related arc.

The Ionian slab further retreated during the second episode of slab-roll back in the southern Tyrrhenian (2–1 Ma), opening the Marsili Basin. The crust of the Marsili Basin is also tholeiitic, however with a stronger arc signature. Ventura et al. (2013) explain the arc-like composition of the Marsili crust and the magmatism of the more recent Marsili Seamount (< 1 Ma) by its location above this former mantle wedge region.

Finally, we note that the area of relatively high velocity north of Corsica, around 43.5°N, 9°E, corresponds to a site of basaltic volcanism related to the opening of the northeastern tip of the Liguro-Provençal Basin 18 Myr ago, as listed by Savelli (2002). Similar to the Vavilov Basin in the Tyrrhenian Sea, this may have been a site of mantle dehydration in the Liguro-Provençal Basin which opened prior to the Tyrrhenian Sea.

In summary, we find that water content is an important factor controlling the shear velocity of the Tyrrhenian Sea in the 70–110 km depth range. Recent mineral physics models that incorporate the effects of hydration-dependent anelastic relaxation predict a sharp drop in shear velocity by the transition from a relatively dry lithosphere to a hydrated asthenosphere (Karato, 2012; Goes et al., 2012; Olugboji et al., 2013), which resembles what we observe for the low-velocity zone of our tomographic model. Such models show that lateral variations in shear velocity of the magnitude we find can be reproduced with reasonable variations in water content (on the order of 500–1000 H/10^6 Si, Goes et al., 2012). Combining this with the tectonic evolution, we conclude that the lateral variations in shallow-mantle shear velocities below the Tyrrhenian region are the expression of hydration by subduction (regions 1, 2 and 4 in Fig. 7) and dehydration by decompressional melting (region 3).

6. The Tyrrhenian Sea and other back-arc basins

Comparison of our results to those for other back-arcs shows some notable similarities and differences. Wiens et al. (2006) determined the average shear-velocity structure of four back-arc basins by waveform modelling using local events. Contrary to our interpretation for the Tyrrhenian Sea region, these authors attribute variations in seismic structure between the basins to variations in mantle potential temperature. Their four 1-D models all show a low-velocity zone with minimum shear velocity at approximately 80 km with minimum values varying from 3.85 (Lau Basin) to 4.15 km/s (Mariana Trough). The increase in minimum velocity from Lau to Fiji to Scotia to Marianas correlates well with increasing mantle temperatures inferred from petrology and basin depth. They rule out variations in water content as an explanation for the inter basin velocity variations because the petrologically inferred water contents increase, rather than decrease, with increasing minimum shear velocity. We note that higher potential temperature means higher melt productivity, which besides generating a larger magmatic crustal thickness that leads to shallower basin depth, would also result in stronger dehydration of the mantle source, which can explain the anti-correlation between temperature and water content found by Wiens et al. (2006). Both temperature and water content may contribute to the velocity structure beneath the four basins studied by Wiens et al. (2006), but variations in temperature apparently dominate the differences between them. In terms of minimum velocity values, the Tyrrhenian shear velocities are most similar to those below the Marianas, where background temperature was inferred to be close to normal MORB-source potential temperature (Wiens et al., 2006), while the other back arcs were all found to be relatively hot.

7. Conclusion

From interstation Rayleigh-wave phase-velocity measurements we constructed a shear-velocity model for the Tyrrhenian Sea region to a depth of about 200 km. Knowledge about the shear-velocity structure is important to understand the mantle processes that accompanied the opening of this back-arc basin. Our shear-velocity model shows a low-velocity zone in the 70 to 110 km depth range surrounding the Vavilov Basin in the southern Tyrrhenian Sea. The low-velocity anomaly is found in, but not only confined to, mantle wedge regions that are characterized by subduction-related volcanism. The geochemical signature of this magmatism provides evidence for the presence of water in their mantle sources. The sharp velocity decrease at 70 km further points to the transition from a relatively dry lithosphere to a more hydrous asthenospheric lower velocity mantle, similar to oceanic settings.

The low-velocity zone is most clearly present beneath the northern Tyrrhenian Sea with a minimum shear velocity of 4.1 km/s at 80 km depth. The northern Tyrrhenian Sea is formed by thinning of its underlying, continental, lithosphere due to roll-back of the Adriatic slab. Whereas slab dehydration and slab retreat must have produced a locally hydrous mantle, most of the region is not characterized by widespread magmatism. Despite the presence of water, the extension apparently did not sufficiently thin the lithosphere to lead to mantle melting and/or to allow any melt produced to reach the surface, except for at a few locations during the opening of the northern Tyrrhenian Sea.

An intriguing aspect of our model is the absence of the low-velocity zone beneath the Vavilov Basin in the southern Tyrrhenian Sea. This oceanic basin was created by strong extension during a period of fast roll-back of the Ionian slab. Whereas decompressional melting due to upwelling might be expected to produce a low shear-velocity anomaly during basin formation, the observation of a relatively high velocity anomaly compared to the surrounding areas suggests an alternative present situation: that of a locally less hydrous mantle. A relatively dry mantle is expected when roll-back occurs fast, because of the large influx of mantle material not affected by subduction. Moreover, extensive melting and the production of the MORB crust will have further dehydrated the underlying mantle during the opening of the basin.

Most of the lateral variations in shear velocity in the 70 to 110 km depth range beneath the Tyrrhenian Sea can therefore be explained by variations in water content. Temperature may also play a role, but the relatively high shear velocity values of the low velocity zone indicate that it may have a smaller effect when compared to other back-arc basins.

Acknowledgements

We used data from the permanent seismic networks MEDNET, Italian Seismic Network, French BB, GEOFON, and IMS, as well as from the CATSCAN, MIDSEA and RETREAT temporary networks. Most data was obtained from the ORFEUS data center, others from the GEOFON data center and IDC. We thank Bill Fry, Läslo Evers and Gert-Jan van der Hazel for help with retrieving data. Processing is based on codes developed by Sergei Lebedev and Thomas Meier and most of the figures were constructed by the Generic Mapping Tools (Wessel and Smith, 1998). We thank the two reviewers for their constructive reviews. The research leading to these results has received funding from Crystal2Plate, an FP7-funded Marie Curie Action under grant agreement number PITN-GA-2008-215353.

Appendix A. Supplementary material

Supplementary material related to this article can be found online at http://dx.doi.org/10.1016/j.epsl.2014.05.028.

References

Argnani, A., Savelli, C., 1999. Cenozoic volcanism and tectonics in the southern Tyrrhenian sea: space–time distribution and geodynamic significance. Geodynamics 27, 409–432.

Avanzinelli, R., Lustrino, M., Mattei, M., Melluso, L., Conticelli, S., 2009. Potassic and ultrapotassic magmatism in the circum-Tyrrhenian region: significance of carbonated pelitic vs. pelitic sediment recycling at destructive plate margins. Lithos 113, 213–227.

Bianchini, G., Beccaluva, L., Siena, F., 2008. Post-collisional and intraplate Cenozoic volcanism in the rifted Apennines/Adriatic domain. Lithos 101, 125–140.

Carminati, E., Lustrino Cuffaro, M., Doglioni, C., 2010. Tectonics, magmatism and geodynamics of Italy: what we know and what we imagine. In: Beltrando, M., Peccerillo, A., Mattei, M., Conticelli, S., Doglioni, C. (Eds.), The Geology of Italy: Tectonics and Life Along Plate Margins. J. Virtual Explorer 36, 59.

Civetta, L., Orsi, G., Scandone, P., Pece, R., 1978. Eastward migration of the Tuscan anatectic magmatism due to anticlockwise rotation of the Apennines. Nature 276, 604–606.

De Astis, G., Kempton, P.D., Peccerillo, A., 2006. Trace element and isotopic variations from Mt. Vulture to Campanian volcanoes: constraints for slab detachment and mantle inflow beneath southern Italy. Contrib. Mineral. Petrol. 151, 331–351.
De Vos, D., Paulssen, H., Fichtner, A., 2013. Finite-frequency sensitivity kernels for two-station surface wave measurements. Geophys. J. Int. 194, 1042–1049.
Dewey, J.F., Helman, M.L., Turco, E., Hutton, D.H.W., Knott, S.D., 1989. Kinematics of the western Mediterranean. In: Coward, M.P., Dietrich, D., Park, R.G. (Eds.), Alpine Tectonics. In: Geol. Soc. Spec. Publ., vol. 45, pp. 265–283.
Di Stefano, R., Kissling, E., Chiarabba, C., Amato, A., Giardini, D., 2009. Shallow subduction beneath Italy: three-dimensional images of the Adriatic–European–Tyrrhenian lithosphere system based on high-quality P wave arrival times. J. Geophys. Res. 114, B05305. http://dx.doi.org/10.1029/2008JB005641.
Faccenna, C., Funiciello, F., Civetta, L., D'Antonio, M., Moroni, M., Piromallo, C., 2007. Slab disruption, mantle circulation, and the opening of the Tyrrhenian basins. Spec. Pap., Geol. Soc. Am. 418, 153–169.
Faccenna, C., Piromallo, C., Crespo-Blanc, A., Jolivet, L., Rossetti, F., 2004. Lateral slab deformation and the origin of the western Mediterranean arcs. Tectonics 23, TC1012. http://dx.doi.org/10.1029/2002TC001488.
Faul, U.H., Jackson, I., 2005. The seismological signature of temperature and grain size variations in the upper mantle. Earth Planet. Sci. Lett. 234, 119–134.
Fischer, K.M., Ford, H.A., Abt, D.L., Rychert, C.A., 2010. The lithosphere–asthenosphere boundary. Annu. Rev. Earth Planet. Sci. 38, 551–575.
Frezotti, M.L., Reccerillo, A., Panza, G., 2009. Carbonate metasomatism and CO_2 lithosphere–asthenosphere degassing beneath the Western Mediterranean: an integrated model arising from petrological and geophysical data. Chem. Geol. 262, 108–120.
Giacomuzzi, G., Chiarabba, C., De Gori, P., 2011. Linking the Alps and Apennines subduction systems: new constraints revealed by high-resolution teleseismic tomography. Earth Planet. Sci. Lett. 301, 531–543.
Giacomuzzi, G., Civalleri, M., De Gori, P., Chiarabba, C., 2012. A 3D Vs model of the upper mantle beneath Italy: insight on the geodynamics of central Mediterranean. Earth Planet. Sci. Lett. 335–336, 105–120.
Goes, S., Armitage, J., Harmon, N., Smith, H., Huismans, R., 2012. Low seismic velocities below mid-ocean ridges: attenuation versus melt retention. J. Geophys. Res. 117, B12403. http://dx.doi.org/10.1029/2012JB009637.
Goes, S., Giardini, D., Jenny, S., Hollenstein, C., Kahle, H.-G., Geiger, A., 2004. A recent tectonic reorganization in the south-central Mediterranean. Earth Planet. Sci. Lett. 226, 335–345.
Gueguen, E., Doglioni, C., Fernandez, M., 1998. On the post-25 Ma geodynamic evolution of the western Mediterranean. Tectonophysics 298, 259–269.
Hirschmann, M.M., 2010. Partial melt in the oceanic low-velocity zone. Phys. Earth Planet. Inter. 179, 60–71.
Jolivet, L., Faccenna, C., Piromallo, C., 2009. From mantle to crust: stretching the Mediterranean. Earth Planet. Sci. Lett. 285, 198–209.
Karato, S., 2012. On the origin of the asthenosphere. Earth Planet. Sci. Lett. 321–322, 95–103.
Karato, S., Jung, H., 1998. Water, partial melting and the origin of the seismic low-velocity and high attenuation zone in the upper mantle. Earth Planet. Sci. Lett. 157, 193–207.
Kennett, B.L.N., Engdahl, E.R., Buland, R., 1995. Constraints on seismic velocities in the earth from travel times. Geophys. J. Int. 122, 108–124.
Lucente, F.P., Chiarabba, C., Cimini, G.B., 1999. Tomographic constraints on the geodynamic evolution of the Italian region. J. Geophys. Res. 104, 20307–20327.
Lustrino, M., Duggen, S., Rosenberg, C.L., 2011. The Central–Western Mediterranean: anomalous igneous activity in an anomalous collisional tectonic setting. Earth Planet. Sci. Lett. 104, 1–40.
Malinverno, A., Ryan, W.F.B., 1986. Extension in the Tyrrhenian Sea and shortening in the Apennines as result of arc migration driven by sinking of the lithosphere. Tectonics 5, 227–245.
Marone, F., van der Lee, S., Giardini, D., 2004. Three-dimensional upper-mantle S-velocity model for the Eurasia–Africa plate boundary region. Geophys. J. Int. 158, 109–130.
Meier, T., Dietrich, K., Stockhert, B., Harjes, H.P., 2004. One-dimensional models of shear-wave velocity for the eastern Mediterranean obtained from the inversion of Rayleigh-wave phase velocities and tectonic implications. Geophys. J. Int. 156, 45–58.
Molinari, I., Morelli, A., 2011. EPcrust: a reference crustal model for the European Plate. Geophys. J. Int. 185, 352–364.
Nikogosian, I.K., Van Bergen, M.J., 2010. Heterogeneous mantle sources of potassium-rich magmas in central-southern Italy: melt inclusion evidence from Roccamonfina and Ernici (Mid Latina Valley). J. Volcanol. Geotherm. Res. 197, 279–302.
Olugboji, T.M., Karato, S., Park, J., 2013. Structures of the oceanic lithosphere–asthenosphere boundary: mineral-physics modeling and seismological signatures. Geochem. Geophys. Geosyst. 14. http://dx.doi.org/10.1002/ggge.20086.
Paige, C., Saunders, M., 1982. LSQR: an algorithm for sparse linear equations and sparse least squares. ACM Trans. Math. Softw. 8, 43–71.
Panza, G.F., Peccerillo, A., Aoudia, A., Farina, B., 2007. Geophysical and petrological modelling of the structure and composition of the crust and upper mantle in complex geodynamic settings: the Tyrrhenian Sea and surroundings. Earth-Sci. Rev. 80, 1–46.
Peccerillo, A., 2005. Plio-Quaternary Volcanism in Italy: Petrology, Geochemistry, Geodynamics. Springer-Verlag, Berlin, p. 365.
Pedersen, H.A., 2006. Impacts of non-plane waves on two-station measurements of phase velocities. Geophys. J. Int. 165, 279–287.
Piromallo, C., Morelli, A., 2003. P wave tomography of the mantle under the Alpine–Mediterranean area. J. Geophys. Res. 108 (B2), 2065. http://dx.doi.org/10.1029/2002JB001757.
Rosenbaum, G., Gasparon, M., Lucente, F.P., Peccerillo, A., Miller, M.S., 2008. Kinematics of slab tear faults during subduction segmentation and implications for Italian magmatism. Tectonics 27, TC2008. http://dx.doi.org/10.1029/2007TC002143.
Rosenbaum, G., Lister, G.S., 2004. Neogene and Quaternary rollback evolution of the Tyrrhenian Sea, the Apennines, and the Sicilian Maghrebides. Tectonics 23, TC1013. http://dx.doi.org/10.1029/2003TC001518.
Rychert, C.A., Shearer, P.M., 2009. A global view of the lithosphere–asthenosphere boundary. Science 324, 495–498.
Savelli, C., 2002. Time–space distribution of magmatic activity in the western Mediterranean and peripheral orogens during the past 30 Ma (a stimulus to geodynamic considerations). J. Geodyn. 34, 99–126.
Schivardi, R., Morelli, A., 2011. EPmantle: a 3-D transversely isotropic model of the upper mantle under the European Plate. Geophys. J. Int. 185, 469–484.
Schmerr, N., 2012. The Gutenberg discontinuity: melt at the lithosphere–asthenosphere boundary. Science 335, 1480–1483.
Schmid, C., van der Lee, S., VanDecar, J.C., Engdahl, E.R., Giardini, D., 2008. Three-dimensional S velocity of the mantle in the Africa–Eurasia plate boundary region from phase arrival times and regional waveforms. J. Geophys. Res. 113, B03306. http://dx.doi.org/10.1029/2005JB004193.
Spakman, W., Wortel, M.J.R., 2004. A tomographic view on the Western Mediterranean geodynamics. In: Cavazza, W., Roure, F., Spakman, W., Stampfli, G., Ziegler, P. (Eds.), The TRANSMED Atlas, The Mediterranean Region from Crust to Mantle, pp. 31–52.
Stixrude, L., Lithgow-Bertelloni, C., 2005. Mineralogy and elasticity of the oceanic upper mantle: origin of the low-velocity zone. J. Geophys. Res. 110, B03204. http://dx.doi.org/10.1029/2004JB002965.
Tesauro, M., Kaban, M., Cloetingh, S.A.P.L., 2008. EuCRUST-07: a new reference model for the European crust. Geophys. Res. Lett. 35, L05313. http://dx.doi.org/10.1029/2007GL032244.
Trua, T., Serri, G., Marani, M.P., 2007. Geochemical features and geodynamic significance of the southern Tyrrhenian backarc basin. Spec. Pap., Geol. Soc. Am. 418, 221–233.
Ventura, G., Milano, G., Passaro, S., Sprovieri, M., 2013. The Marsili Ridge (Southern Tyrrhenian Sea, Italy): an island-arc volcanic complex emplaced on a 'relict' back-arc basin. Earth-Sci. Rev. 116, 85–94.
Wessel, P., Smith, W.F.H., 1998. New, improved version of generic mapping tools released. EOS Trans. AGU 79 (47), 579.
Wiens, D.A., Kelley, K.A., Plank, T., 2006. Mantle temperature variations beneath back-arc spreading centers inferred from seismology, petrology, and bathymetry. Earth Planet. Sci. Lett. 248, 30–42.
Wortel, M.J.R., Spakman, W., 2000. Subduction and slab detachment in the Mediterranean–Carpathian region. Science 290, 1910–1917.
Zhu, H., Bozdağ, E., Peter, D., Tromp, J., 2012. Structure of the European upper mantle revealed by adjoint tomography. Nat. Geosci. 5, 493–498.